

IS CRYOPRESERVATION SUPERIOR OVER TANNIC ACID/ARGININE/OSMIUM TETROXIDE NON-COATING PREPARATION IN FIELD EMISSION SCANNING ELECTRON MICROSCOPY?

W.L. Jongebloed*, I. Stokroos, D. Kalicharan and J.J.L. van der Want

Laboratory for Cell Biology and Electron Microscopy, University of Groningen, The Netherlands

(Received for publication April 22, 1998 and in revised form September 22, 1998)

Abstract

Rat kidney tissue was prepared for field emission scanning electron microscope (FE-SEM) observation, either by *chemical fixation* or by *cryofixation*. Chemical fixation was carried out by glutaraldehyde prefixation followed by tannic acid/arginine/osmium tetroxide *non-coating* postfixation procedure, dehydration and critical point drying from liquid CO₂. Cryofixation was carried out by slam-freezing on a copper mirror in liquid N₂ of either vibratome sections of very mildly prefixed tissue or of small tissue blocks, some of which were infiltrated with 10-15 % glycerol. In half of the specimens glycerol was removed by substitution in the cold. Non-cryo-protected samples showed slightly more ice-crystal damage than cryo-protected specimens. The cytoplasmic information obtained from cryo-images after mild prefixation, with or without glycerol or butanol, respectively, is very much comparable with that of transmission electron microscope images of the same structures. *Non-coating* images investigated at 2-3 kV gave the best three-dimensional information, but also showed structural details at cell surfaces. These different preparation methods provided complementary fine structural information on the kidney. A combination of cryo- and *non-coating* preparation/ observation is highly desirable, particularly with relatively less known structures.

Key Words: Field emission scanning electron microscopy, cryo field emission scanning electron microscopy, kidney, tannic acid/arginine/osmium tetroxide non coating, glycerol, *t*-butanol.

*Address for correspondence

W.L. Jongebloed
Laboratory for Cell Biology and Electron Microscopy
University of Groningen
Oostersingel 69/2
9713 EZ Groningen, The Netherlands
FAX Number: +31-50-3632515
E-mail: w.l.jongebloed@med.rug.nl

Introduction

Tissues can be prepared either by *chemical fixation* including dehydration and subsequent drying (critical point or freeze drying), or alternatively by *cryo-fixation* and subsequent observation at low temperature.

Chemical fixation

Optimal visualization of the morphology in field emission scanning electron microscopy (FE-SEM) after *chemical fixation* is dependent on a number of factors such as the preservation of the various components, dehydration and drying of the sample and the accelerating voltage employed. FE-SEMs require optimally prepared samples at both low and high acceleration voltages, because preparation artefacts become easily observable due to the high resolution (Ansell and Capers, 1989). FE-SEMs in the standard configuration can produce 5 kV images of biological specimens with the same resolution as obtained with a tungsten (W) or a LaB₆ cathode at 15-25 kV. In-lens and semi-in-lens instruments can produce even higher resolution images, particularly in the low kV range.

Chemical fixation can either be carried out as standard glutaraldehyde (GA)/osmium tetroxide (OsO₄) fixation or as glutaraldehyde plus additives for the *non-coating* procedure. In both cases a mixture of glutaraldehyde/paraformaldehyde/acrolein as prefixation can be used as well.

Standard chemical fixation. Standard fixation is traditionally carried out by means of a GA prefixation, by perfusion and subsequent immersion fixation or immersion fixation only, followed by OsO₄ postfixation. Because of the poor electrical conductivity, a thin conductive coating has to be applied before observation in the (FE-) SEM. The thickness of the layer, the kind of coating material (e.g., Cr, Pt, Au/Pd) and its grain size, as well as the sputtering procedure are very important factors in the production of possible artificial structures on the specimen surface and play an important role in the eventual visualization of the fine structure (Wepf *et al.*, 1991; Wergin *et al.*, 1993; Apkarian, 1994; Stokroos *et al.*, 1998).

The OsO₄ penetration in the specimen is relatively slow, with consequences for the bulk preservation and conductivity, which results in an inferior final resolution. Due to the rather poor preservation, extraction of certain constituents can occur during the various rinsing and dehydration steps (Jongebloed *et al.*, 1996). Moreover, critical point drying (CPD) and to a lesser extent freeze-drying (FD), can cause shrinkage, influencing the spatial relations of the structures to be investigated in the SEM.

Freeze-drying is often carried out from *t*-butanol, to avoid freeze artefacts due to ice crystal formation. Edelmann (1994) used low temperature exchange of freeze-dried material, while Allenspach (1993) used acetone as a medium containing either uranyl acetate, acrolein with tannic acid or acrolein alone, tannic acid, OsO₄ and GA. Gilkey and Staehelin (1986) have compared the results of cryo-fixation and chemical fixation, although their investigation concerned *standard* (GA + OsO₄) fixation versus *cryo*-fixation.

Non-coating chemical fixation. A considerable improvement in the preservation of the tissue constituents and the overall sample conductivity is obtained by the use of non-coating procedures as mordant/postfixation. These methods make use of either thiocarbohydrazide (Murphy, 1978; Jongebloed *et al.*, 1992a,b; Kalicharan *et al.*, 1992), or alternatively, tannic acid (Murakami, 1974; Chaplin, 1985; Jongebloed and Kalicharan, 1992, 1994; Jongebloed *et al.*, 1993a,b, 1994) as a ligand to enhance osmium bonding and fixation.

Thiocarbohydrazide is often used with tissue, already fixed according to the standard (GA + OsO₄) method in combination with OsO₄, in the so-called OTO (osmium/thiocarbohydrazide/osmium) or OTOTO (osmium/thiocarbohydrazide/osmium/-thiocarbohydrazide-osmium) method (Jongebloed and Kalicharan, 1992; Jongebloed *et al.*, 1992b). Thiocarbohydrazide can, if bound to an already osmicated structure, bind other osmium molecules and so enhance sample conductivity and generation of secondary electrons.

Tannic acid or galloyl glucose is often used with GA prefixed samples in combination with arginine and OsO₄; this is the TAO (tannic acid/arginine/OsO₄) method, which is very effective for the preservation of various (acid) mucopolysaccharides and glycoproteins (Los *et al.*, 1992; Kalicharan *et al.*, 1992; Dunnebie *et al.*, 1995; Jongebloed *et al.*, 1996; Jongebloed and Kalicharan, 1996). Galloyl glucose has various reactive groups such as hydroxyl, carboxyl and sulfonic groups, which bind in different ways to amino acids, hyaluronic acid, glycoproteins, lysine, collagen and arginine and also can bind heavy metal ions such as osmium, uranyl and ruthenium. In a way tannic acid is more widely

applicable than thiocarbohydrazide. Tannic acid can also be used after standard GA fixation in combination with OsO₄ or uranyl. The appearance of the image is more like standard transmission electron microscopy (TEM) images, although the conductivity in FE-SEM is poor, requiring a conductive coating. This application of tannic acid however, did not gain much support. OTO, OTOTO and TAO combination are most suitable for a variety of types of specimens/ structures.

As a result of the superior fixation by non-coating treatments, extraction of constituents is minimized compared to the conventional GA/OsO₄ fixation method mentioned before.

Chemical fixation, either conventional or *non-coating*, is rather time consuming if the sample has to be transferred from one solution to another. If fixation is carried out in a microwave oven (Kok and Boon, 1992; Jongebloed and Kalicharan, 1994; Login and Dvorak, 1994a,b), the chemical fixation procedure can be carried out in about 1 hour at 35-45°C. Since CPD or FD requires another 30-60 minutes real time, the whole preparation procedure takes 90-120 minutes; on the other hand screening times are also in this order of magnitude.

Cryofixation

Optimal visualization of the morphology in FE-SEM after *cryo fixation* is strongly dependent on the size of the specimen, the freezing procedure, the use of a cryo-protectant and/or a very mild prefixation and even the type of cryo-transfer system employed. For TEM investigation, *cryo-fixation* and subsequent freeze fracturing/etching and replication is a well-known method, giving an almost similar result as cryo-FE-SEM. The advantage of the freeze replication method is the slightly higher resolution of the TEM, the disadvantages are the loss of the specimen and the risk to contaminate the replica with specimen debris.

Several investigators have shown the advantages of cryo-preservation and observation of biological tissues and structures (Inoué, 1985; Inoué and Koike, 1986; Finch *et al.*, 1987; Walther *et al.*, 1990; Guggenheim *et al.*, 1991; Allenspach, 1993; Hohenberg *et al.*, 1994).

Cryomethods for SEM and TEM have been used by various investigators, mainly because chemical fixation, rinsing and dehydration steps can extract certain components, as discussed before. In addition, drying methods, such as critical point and freeze drying, can cause volume changes, due to shrinkage as described by others (Echlin and Burgess, 1977; Echlin, 1978, 1992; Boyde and Maconnachie, 1979; Sargent, 1986, 1988).

Cryotechniques, whether used for TEM or SEM have been used in the past in various fields of interest, such as plant pathology, viruses, dairy industry, food

systems, biopolymers (Willison and Rowe, 1980; Sargent, 1986; Adrian *et al.*, 1984; Robards and Sleytr, 1985; Talmon, 1986; Frederik *et al.*, 1989; Humphreys, 1989; Van Aelst *et al.*, 1989; Echlin, 1992; Robards and Abeysekera, 1992; Kalab, 1993; Zhang and Rawson, 1993, 1996).

One of the main problems involved in cryotechniques is the occurrence of crystalline ice, mainly due to slow freezing. All cryo techniques mentioned before, either for SEM or TEM, have to deal with this problem (Müller *et al.*, 1980; Carr *et al.*, 1983; Gilkey and Staehelin, 1986; Sitte *et al.*, 1987).

There are two possibilities to avoid or at least to slow down the formation of crystalline ice: infiltration with a cryoprotectant and/or a preliminary very mild prefixation.

Freezing at atmospheric pressure. Pure water in the solid state (ice) can be present as vitreous, cubic or hexagonal ice; both cubic and hexagonal ice are crystalline, while vitreous ice is amorphous. Slow freezing promotes the existence of cubic or hexagonal ice crystals. The electron microscopist probably will not observe cubic ice, because it quickly transforms into hexagonal ice. Due to the temperature gradient occurring in the sample at the moment it is cooled down in liquid N₂, crystalline ice will appear and damage cell membranes causing artefactual structures; therefore the cooling speed is of eminent importance. When the water is cooled fast enough vitreous ice is formed. On the other hand when vitreous ice is warmed up slowly, it transforms through cubic ice to hexagonal ice; the transition temperatures are -121°C and -80°C (Reid and Beesely, 1991). Moreover, because biological material is a poor thermal conductor it is likely that crystalline ice will be formed in the inner layers of the sample.

Various methods to freeze samples of different origin and size at atmospheric pressure have been developed and are extensively described by Robards and Sleytr (1985).

To protect the tissue/material against freeze artefacts, infiltration of a cryoprotectant or a mild prefixation prior to freezing or a combination of both are highly recommended (Meissner and Schwartz, 1990).

Freezing at high pressure in a closed system. High pressure freezing can (partially) avoid ice crystallization and although the system is not generally in use yet, because of the rather high investment involved, it nevertheless seems highly prospective. When water is pressurized to 2.1×10^8 Pa, the freezing point is lowered to -22°C and in consequence the critical cooling rate for vitrification is reduced to 2×10^4 K per second for water and to 10 K per second for biological tissue, reducing nucleation rate and ice crystal growth (Robards

and Sleytr, 1985; Humbel and Müller, 1986; Moor, 1987; Studer *et al.*, 1989). Almost over the full width of the sample (approximately 200-500 mm) the formation of crystalline ice can be avoided to a large extent.

Both fast freezing at atmospheric pressure and high pressure can be used in combination with either infiltration of a cryoprotectant or a preliminary very mild prefixation as mentioned before. By fast freezing at atmospheric pressure it is possible to minimize ice crystal artifacts by vitrification of water, but only 10-20 mm of an unfixed tissue sample are effectively frozen (Plattner and Bachmann, 1982; Menco, 1986; Dubochet *et al.*, 1991). The last mentioned authors claim that with very fast freezing rates, the volume with almost no crystalline ice can extend to approximately 100 mm from the surface first in contact with the cooling face.

In our study we employed fast freezing at atmospheric pressure on a pre-cooled mirror, using vibratome sections of tissue, which were either very mildly fixed with glutaraldehyde or infiltrated with glycerol as cryoprotectant, prior to freezing. Prior to the freezing step, the vibratome sections were mounted on a TEM copper grid; we call this method the *grid method*. Cryofixation and observation of frozen samples with the FE-SEM is a fast method, images can be obtained within approximately 20 minutes after excision of tissue from patient or animal.

The purpose of the investigation was to compare images of kidney fine structure obtained with FE-SEM either after *cryofixation* (mild GA prefixation or infiltration with glycerol respectively) or *chemical fixation* (GA/tannic acid/arginine/OsO₄ non-coating method).

Materials and Methods

Cryoprotectant infiltration method

Fresh tissue blocks (approximately 1x1x1 mm³) or vibratome sections (250-300 mm) of rat kidney in buffer solution were infiltrated with 10-15 % glycerol or not infiltrated at all and subsequently slam-frozen against a copper mirror of a Balzers (Liechtenstein) KF 80 at -196°C in liquid N₂. The frozen samples were, with or without removal of the glycerol in the cold, transferred to an Oxford Instruments (Oxford, UK) 1500 HF cryotransfer system connected to the FE-SEM. After fracturing, the samples without glycerol cryoprotection were ice sublimated for 60 seconds at -110°C. All samples were subsequently sputter-coated with approximately 3-4 nm Au/Pd with the built-in planar magnetron sputtering device (Denton/Oxford, Witney, UK) at cryo temperature. Samples were finally transferred to a JEOL (Tokyo, Japan) 6301F FE-SEM; observations were carried out at 5-10 kV.

Prefixation - grid method

Rat kidney was perfused for 1 min with 0.1 M sodium cacodylate buffer, containing 2% PVP (polyvinylpyrrolidone; MW 40000) and 75 mM NaNO₂ and heparin, and subsequently fixed by perfusion with buffered 0.1% GA (pH 7.4) for 5 min. To stop the fixation, the tissue was rinsed in the same buffer solution. Vibratome sections (100 μm) of the mildly prefixed tissue, were placed onto 3.0 mm (75 mesh) copper grids, attached to a slammer holder, whereafter the excess of buffer solution was removed with filter paper. Grid and tissue hanging up-side down were slammed against the mirror of the Balzers KF 80 at -196°C. Under liquid N₂, the grid with tissue was detached from the holder and placed into the slot of a Balzers cryo-holder and subsequently transferred to the cryo-transfer system connected to the FE-SEM. The upper part of the copper grid was bent away, exposing the tissue. Subsequently the samples were fractured and the ice was sublimed for 60 seconds at -110°C. Finally the freshly obtained surfaces were sputter coated with a 3-4 nm Au/Pd by the built-in magnetron sputter coater. The samples were then transferred to the FE-SEM; observations were carried out at 5-10 kV.

SEM-TAO non-coating method

Rat kidney was perfused for 5 min with 0.1 M sodium cacodylate buffer, containing 2% PVP and 75 mM NaNO₂ and heparin and subsequently fixed by perfusion with 2% GA (pH 7.4; 15 minutes) in the same buffer. Following excision, the kidney was fixed by immersion overnight in 2% GA in the same buffer (pH 7.4; 400 mM; 4°C); subsequently, 100 μm vibratome sections were produced. After rinsing in buffer solution (3 x), the tissue blocks were immersed in a mixture of arginine-HCl, glycine, sucrose and sodium glutamate (2% each; 16 hours; room temperature [RT]), followed by rinsing in distilled water (3x). Subsequently samples were immersed in a mixture of tannic acid and guanidine-HCl (2% each; 8 hours; RT) and rinsed in distilled water (3x). After immersion in 2% OsO₄ solution in distilled water (8 hours; 20°C) and subsequent rinsing in distilled water (3x), as described previously (Jongebloed *et al.*, 1996). Specimens were dehydrated in an ethanol series with concentrations increasing to 100%, subsequently dried by CPD in liquid CO₂ and investigated in the JEOL FE-SEM, operated at 2-3 kV.

SEM-prefixation-cryomethod with *t*-butanol

Up till the GA immersion fixation overnight and the production of vibratome sections, rat kidney was prepared similarly to the non-coating procedure described in the previous section. After rinsing in buffer solution (3x), samples were dehydrated in an ethanol series, etha-

Figures 1-2. Type A: Tissue frozen without cryoprotectant infiltration or mild 0.1M GA- pre-fixation (Figs. 1 and 2), showing ice-crystal damage. **Figure 1.** Distal tubular cell with infoldings (if), mitochondria (mt) with their cristae and short microvilli; bar = 2 μm. **Figure 2.** Glomerular capillary system with basal membrane (bm), podocytes (po) and capsule of Bowman (cb); bar = 2μm.

Figures 3-6. Type B: Tissue frozen with glycerol cryoprotectant infiltration, but without mild 0.1 M GA-pre-fixation, showing decrease of detail in information due to the presence of glycerol. **Figure 3.** Proximal tubular cells with microvilli (mi) extending in lumen (lu); bar = 18 μm = 5 μm. **Figure 4.** Detail of apical brush border of microvilli (mi); bar = 22 μm = 2 μm. **Figure 5.** Nucleus with inner (one arrow) and outer (two arrows) membrane with nuclear pores; bar = 11 μm = 2 μm. **Figure 6.** Flattened fenestrated capillary endothelium of glomerulus, pores (po) filled with glycerol; bar = 22 μm = 2 μm.

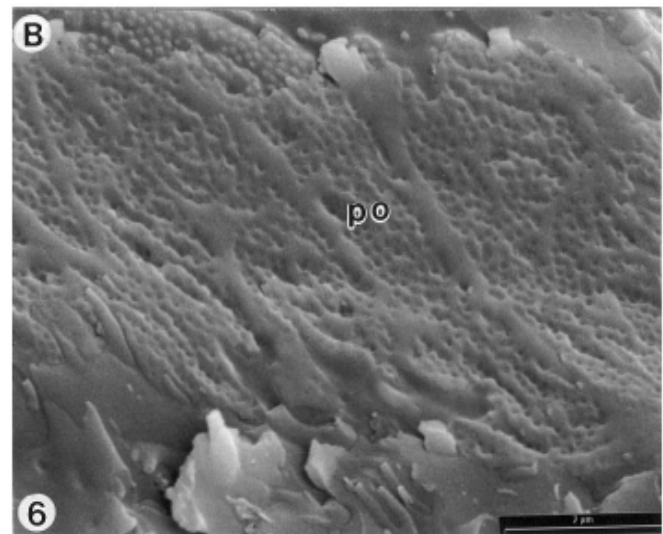
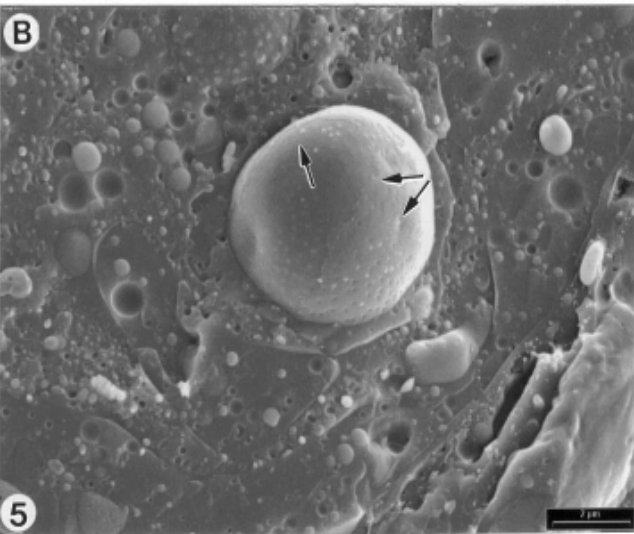
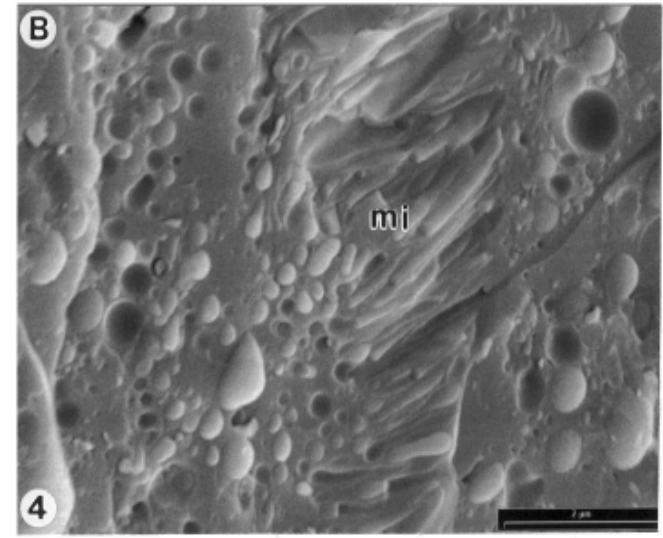
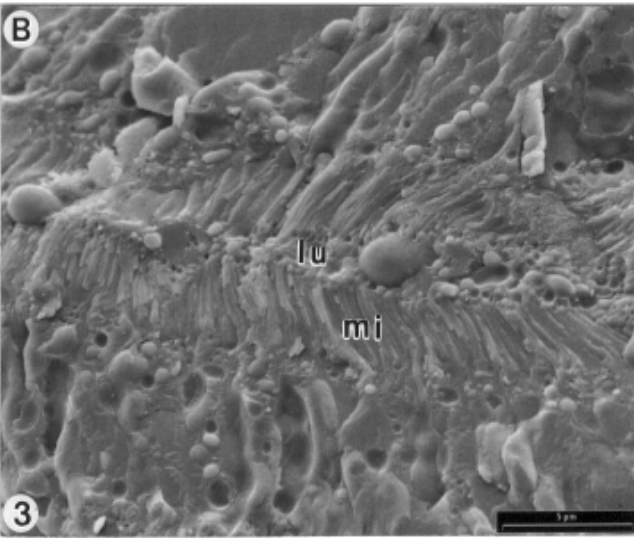
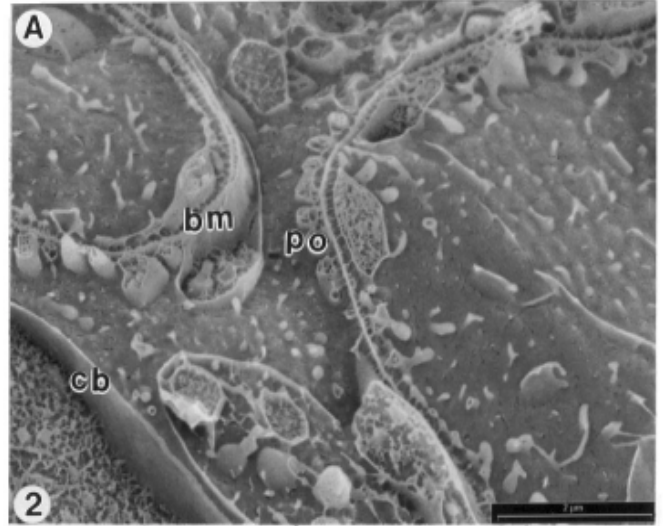
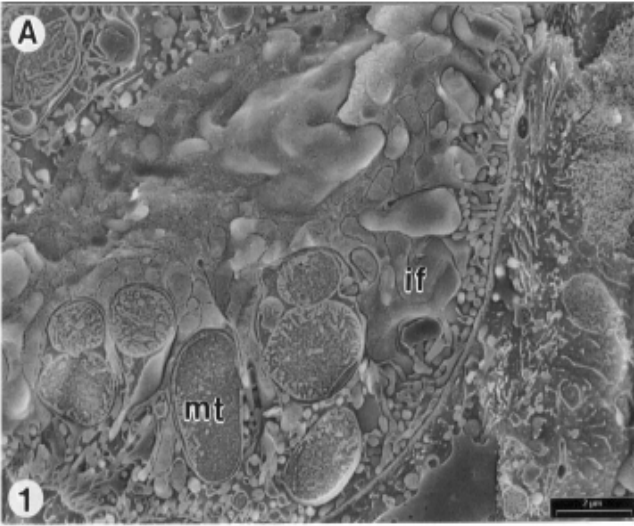
nol was exchanged for 100% *t*-butanol. Subsequently the samples were treated similar to the “grid-method” as described above.

Results

The following series of experiments was carried out on rat kidney tubular and glomerulus structures for comparison of the morphology after a number of preparation procedures for cryo-FE-SEM and the tannic acid/arginine/osmium tetroxide procedure including dehydration and drying for FE-SEM as well:

- A. Tissue frozen without cryo-protectant infiltration and without mild pre-fixation.
 - B. Tissue frozen with glycerol infiltration, but without mild pre-fixation.
 - C. Tissue frozen with glycerol infiltration and mild pre-fixation.
 - D. Tissue frozen without glycerol infiltration, but with mild pre-fixation.
 - E. Tissue frozen with 30-100% *t*-butanol infiltration after standard 2% GA pre-fixation, *t*-butanol was removed by sublimation at -110°C.
 - F. Tissue fixed after standard GA pre-fixation and TAO non-coating post-fixation, dehydration and CPD.
- Procedure E is different from the others, because the sample is observed in the frozen state, but the specimen received a full GA fixation similar to that of *non-coating* after which infiltration with 30-100% *t*-butanol was performed. Procedure F represents the standard GA *non-coating* procedure, including dehydration and drying.

Cryopreparation for FESEM



Procedure A: Without cryo-protectant, without mild pre-fixation

In the fractured distal tubulus (Fig. 1), the basal membrane with the infoldings of the tubular cells can be observed; in the extracellular space, freeze damage is detectable. The cytoplasm contains rather well preserved cell organelles such as mitochondria with their cristae and the nucleus. At the apical surface of the cell some short microvilli are observable. Figure 2 shows a fracture through the capillary system of a glomerulus, surrounded by the capsule of Bowman, with the basal membrane and attached podocytes. The wall of the blood capillary is covered with remnants of endothelial cells; these cells as well as the pedicles of the podocytes are considerably damaged due to ice crystal formation.

Procedure B: With glycerol, but without mild GA-prefixation

Figure 3 demonstrates adjacent proximal tubular cells with their microvilli extended into a small lumen; note the many vacuoles in and outside the cytoplasm. The visibility of the microvilli is somewhat obscured because of the presence of glycerol, the same is true for the infoldings of the cells. A detail of the apical side of a microvillous brush-border is observable in Figure 4. The fracture occurred not across the cell organelles, but along their exterior, that is, through the ice phase, showing the positive and negative imprints of the cytoplasmic contents. Another fracture in the neighborhood of the cell nucleus (Fig. 5), shows the inner and outer nuclear membrane with their pores. The cytoplasm does not reveal much information, similar to Figure 4. A fracture through the endothelium of a blood capillary of the glomerulus is seen in Figure 6. Apparently the whole surface of the fenestrated endothelium seems flattened and smooth, due to the glycerol infiltration of the pores.

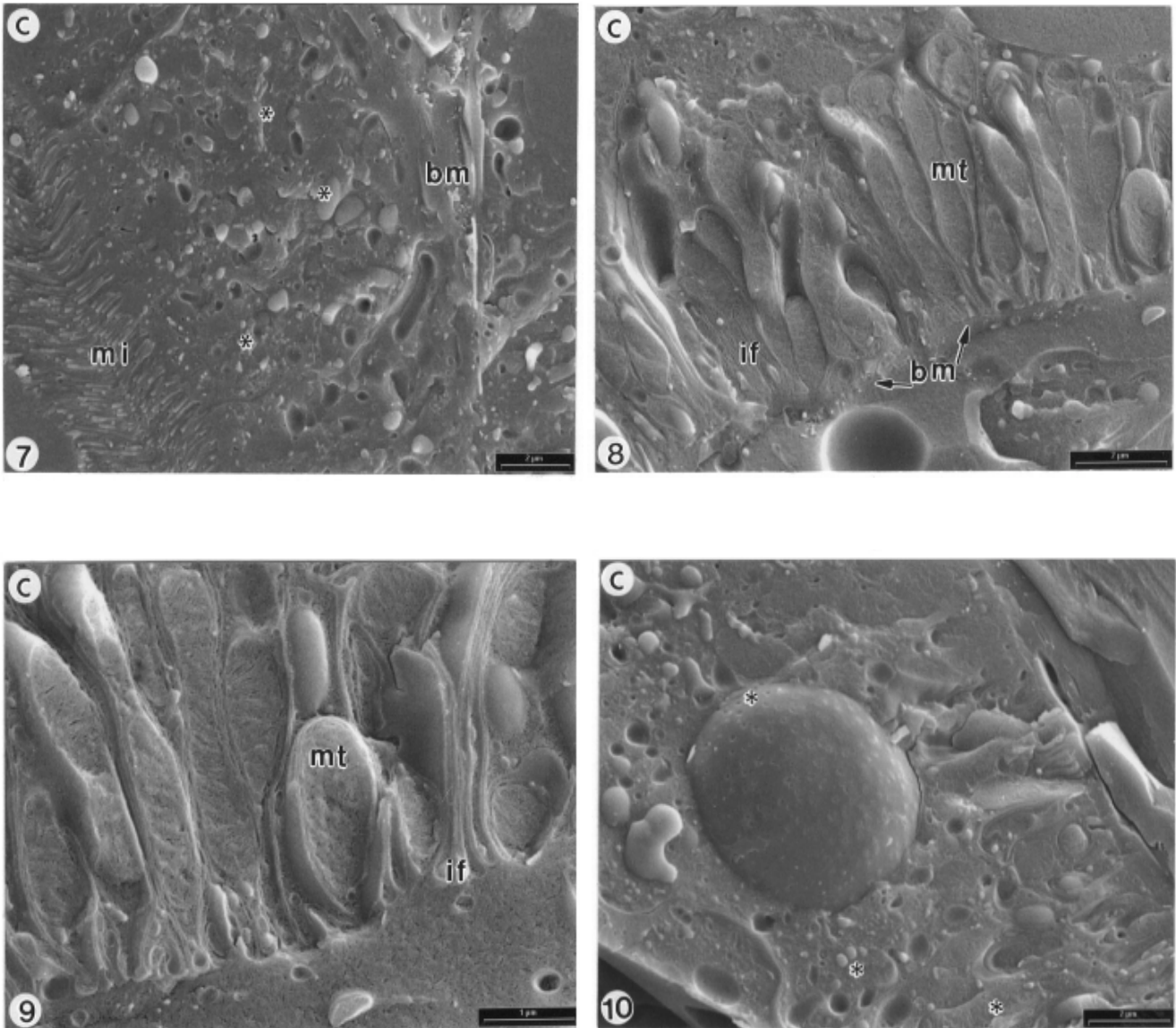
Procedure C: With glycerol infiltration and mild GA-pre-fixation

Figure 7 represents a low magnification of proximal tubular cells. At the apical side the microvilli brush border is seen, while towards the center the cytoplasmic organelles and, to the right side, the basal membrane, are situated. In Figure 8 a similar cell is fractured through the basal side, showing fractured mitochondria and cell infoldings. The arrangement of the membrane system of the mitochondria is obscured by glycerol infiltration, which does not allow ice sublimation. Figure 9 shows a detail of the basal part of a proximal tubular cell with mitochondria between the infoldings of the plasma membrane. The mitochondrial cristae are noticeable, but the spaces in between the cristae, which are seen both in TEM and in the *non-coating* images are absent. This may be due to the fact that these

spaces are filled with glycerol or even that the image seen here represents the true natural state of mitochondria. Figure 10 shows a distal tubule cell similar to that in Figure 5, but now after a mild GA fixation. The infoldings can be more clearly observed here, but the cytoplasmic vacuoles are less prominent.

Procedure D: Without glycerol, but with mild GA pre-fixation

The grid procedure, as used in all cases of freezing samples, is illustrated in Figures 11 and 12. The specimen holder with vibratome section, grid and spring used for cryo preparation prior to slam freezing can be observed in Figure 11. After freezing, the grid was bent away with the cold knife fracturing the frozen tissue. A detail of the tissue and grid can be seen in Figure 12. It shows that the tissue part, approximately 10 mm, which was slammed against the copper block, appeared smooth in comparison to the part adjacent to the grid, which appeared rough due to ice artefacts. Figure 13 represents a kidney proximal tubular cell; in the cross fracture through this cell, the microvilli are seen mostly in lateral view extending into the lumen filled with frozen buffer solution. The microvilli are fractured in various ways, sometimes just below the top, sometimes showing a somewhat hollowed-out appearance. The apical site of the microvilli can be clearly observed, as can the various cell organelles, such as vesicles, nuclear pores, mitochondria and the cell borders between the various cells. Depending on the ice sublimation time, in this case 60 seconds, the intermediate mass between the various cell organelles has a more or less granular appearance. Figure 14 shows a higher magnification of a similar area of the cytoplasm. The ice sublimation time is 90 seconds here, leading to a better visualization of the various cell organelles, but also to a more granular appearance, possibly the effect of a kind of maceration process as a result of ice sublimation in combination with the mild pre-fixation. Figure 15 represents a cross fracture through a part of a glomerulus, close to the enveloping capsule of Bowman. The pedicles of the podocytes seem less damaged as compared to the sample without mild pre-fixation (Figure 2). The fenestrated endothelium of the capillary wall along the basement membrane appears similar to that seen in the adjoining TEM image. The TEM image of a similar area, Figure 16, prepared according to the TAO *non-coating* procedure and embedded afterwards, demonstrates podocytes with their pedicles and basement membrane. Note that the TEM image is flat compared to the three-dimensional FE-SEM image of Figure 15.



Figures 7-10. Type C: Tissue frozen with glycerol cryoprotection infiltration and mild 0.1 M GA-pre-fixation, showing less damage to cell organelles. **Figure 7.** Proximal tubular cell with microvilli (mi) brushborder, basement membrane (bm) and various cell organelles (*); bar = 11 mm = 2 μ m. **Figure 8.** Similar cell, but fractured at the basement membrane (bm); cell infoldings (if) and mitochondria (mt) with inter-cisternal spaces somewhat obscured due to glycerol infiltration; bar = 14 mm = 2 μ m. **Figure 9.** Detail of mitochondria (mt) and infoldings (if) of the plasma membrane; bar = 14 mm = 1 μ m. **Figure 10.** Distal tubular cell with nucleus with pores and various cell organelles, compare with Figure 5. The mildly fixed specimens show more detail than those prepared with glycerol only; bar = 13 mm = 2 μ m.

Procedure E: With 30-100% *t*-butanol after standard 2% GA-prefixation

Figure 17 shows two glomeruli, they are partly enveloped by the capsule of Bowman. At the right hand corner a number of distal tubuli with their small microvilli is observable. A detail of a glomerulus is shown in

Figure 18, the podocyte cell bodies with their primary, secondary and tertiary extensions can be easily observed as well as the interdigitating pedicles and the filtration slits. A slightly higher magnification of a fractured glomerulus with fenestrated endothelium of a capillary, adjacent to part of the podocyte body with its exten-

sions, can be seen in Figure 19. A detail of the fenestrated endothelium with its thickened branches is shown in Figure 20; the fenestrations are all about the same size. In the pores making up the fenestration, the substructure of the underlying network of fine fibrils is observable. The thicker branches are not completely smooth, but show some porosity which could be the result of *t*-butanol extraction.

Procedure F: Non-coating (2% GA + TAO), dehydration, CPD

Figure 21 represents a glomerulus, partially enveloped by the capsule of Bowman; the podocyte body with its various extensions can be easily observed. A detail of that podocyte body is seen in Figure 22 with its highly branched network of pedicles enclosing the filtration slits. The thicker extensions of the podocyte body also appear as slightly porous. The capillary endothelium with its fenestrations is observable at higher magnification in Figure 23, the thickened branches appear thicker than those in cryo-images after *t*-butanol treatment. The whole picture has a more three-dimensional appearance than that of Figure 20, although in that image the fenestrae appear more regular, possibly drying forces caused shrinkage during specimen preparation. A distal and a proximal tubulus adjacent to each other are observable in Figure 24. The microvilli lining of the proximal tubular cell is covered with all kinds of more or less globular particles. A detail of a distal tubulus is shown in Figure 25. The typical infoldings of the basal membrane are well visible in this image, and so are the microvilli lining the luminal side of the cell. At a few places where the plasma membrane is torn, a view into the cytoplasm is possible. A detail of a distal tubulus with luminal surface covered with short microvilli can be seen in Figure 26.

Discussion

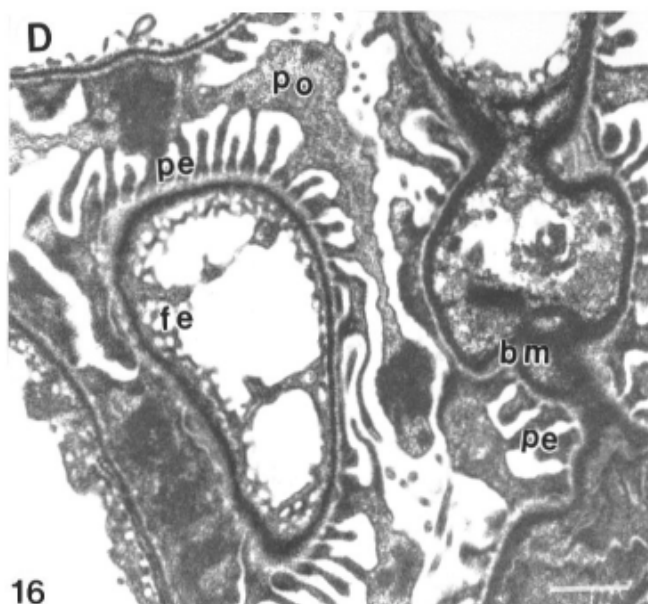
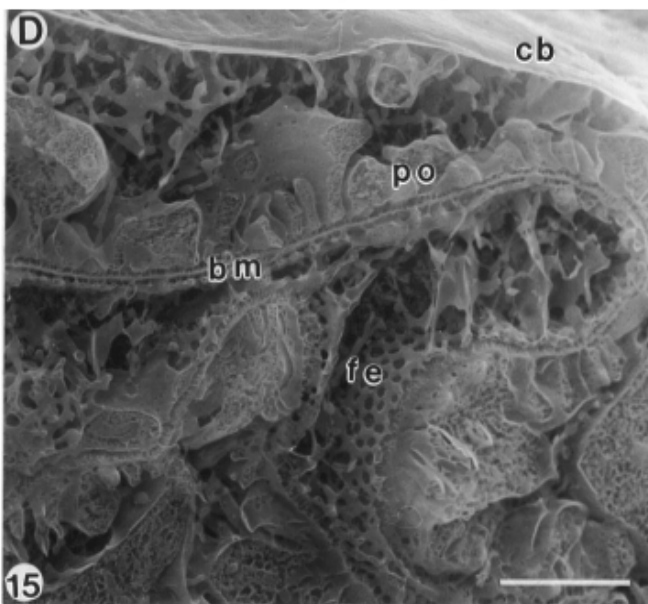
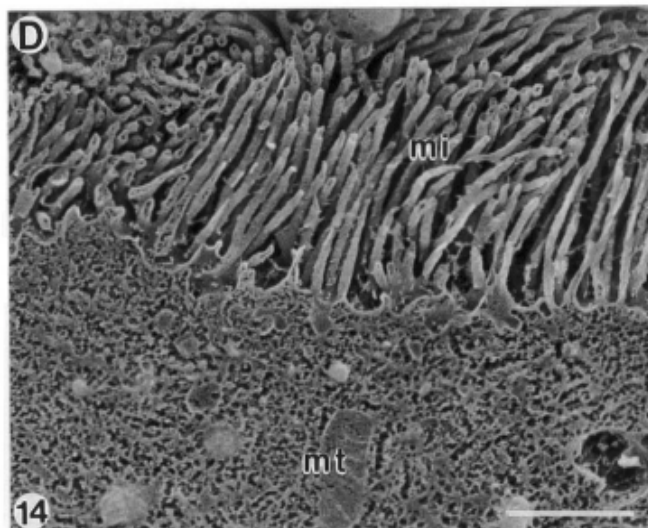
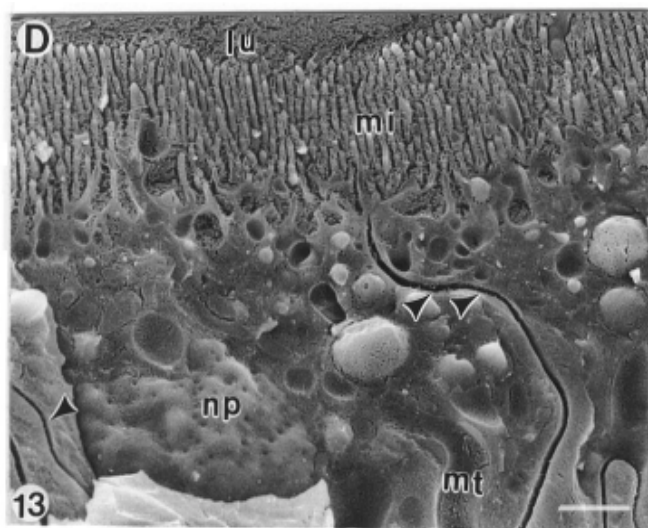
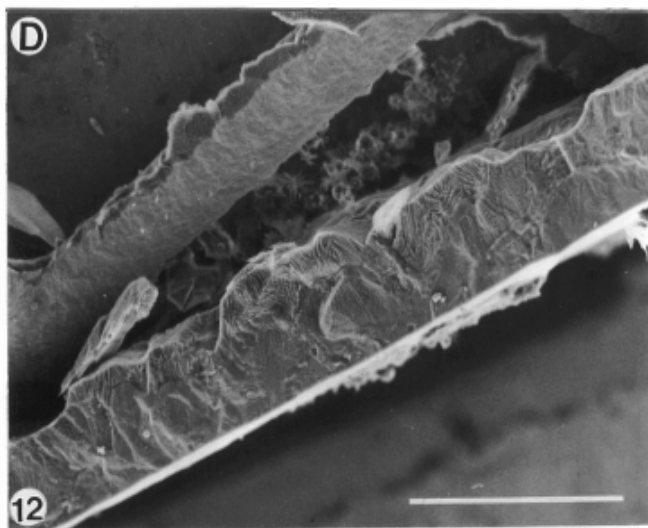
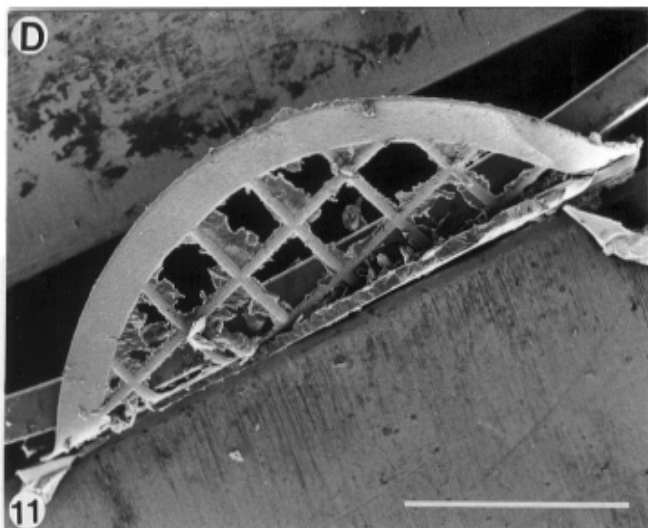
Chemical fixation

Particularly in FE-SEM, whether in standard, in-lens or semi-in-lens configuration, optimal preservation and conductivity are important parameters in obtaining high resolution images. A *non-coating* postfixation according the tannic acid/arginine/osmium tetroxide procedure enhances the uptake of osmium or other heavy metals necessary for optimal preservation and conductivity. There is a disadvantage, though: the binding of tannic acid/osmium to certain structures can lead to large complexes, that disturb the real view of the structure (Los *et al.*, 1992; Jongebloed and Kalicharan, 1996). When a large amount of osmium is bound, maybe in the case with the OTOTO procedure the complexes formed

Figures 11-16. Type D: Tissue frozen without glycerol cryoprotectant infiltration, but with mild pre-fixation showing a better differentiation, but a slightly more pitted appearance due to ice sublimation. **Figures 11-12.** Detailed images of spring, bent away grid and tissue in cryo-holder, as part of the grid-method are shown. Note the smooth fracture surface of the vibratome section closest to the cold slammer block (Fig. 12); bar = 32 mm = 1 mm (Fig. 11); bar = 30 mm = 100 μ m (Fig. 12). **Figure 13.** Proximal tubular cell with microvilli (mi) in lateral view, fractured in different ways; the lumen (lu) is filled with buffer solution; mitochondria (mt), nuclear pores (np) and cell borders (arrowhead) well observable; bar = 10 mm = 1 μ m. **Figure 14.** Detail of cytoplasm of similar cell with mitochondria (mt), microvilli (mi) sometimes appear as hollow tubes; overall structure more pitted; bar = 19 mm = 1 μ m. **Figure 15.** Fractured glomerulus with capsule of Bowman (cb) showing fenestrated capillary endothelium (fe), basement membrane (bm), podocytes (po); bar = 19 mm = 2 μ m. **Figure 16.** TEM image after TAO non-coating treatment, demonstrating podocytes (po) with pedicles (pe), basement membrane (bm) and part of the fenestrated endothelium (fe); bar = 11 mm = 1 μ m.

with osmium can disturb detailed viewing of the structure, particularly in tissue rich in e.g., glycosaminoglycans, mucopolysaccharides, or hyaluronic acid. This can be clearly seen in TEM images of ultrathin sections of OTOTO treated tissues at rather high magnifications (Jongebloed and Kalicharan, 1992). The problem of extraction of certain components during rinsing and dehydration steps, as well as shrinkage, is minimized after TAO and OTOTO non coating treatment, respectively, because of the highly improved preservation of these components (Jongebloed *et al.*, 1996).

The conventional postfixation with OsO₄ only does not optimally preserve the various structures, because of the poor penetration of the osmium. A poor osmium bonding causes an inferior (bulk) conductivity, which is a problem at both high and low accelerating voltages. A thin (2-3 nm) metal coating is sufficient to overcome the lack of conductivity, but not appropriate to improve the preservation or bulk conductivity. Moreover, Au-coatings, even in rather thin layers, can show a substructure, due to agglomeration of Au nuclei. This phenomenon is also strongly dependent on the thickness of the layer, the substrate, the compound, the electrostatic properties of the specimen surface and the sputtering method. This sub-structure disturbs the view onto the specimen surface. Sputtering by means of the so-called magnetron method, in general, is the best way to produce a conduc-



tive coating with a minimum of sub-structure.

In the past Au was employed to coat the sample surface, either after chemical fixation or cryofixation (Inoué, 1985; Van Aelst *et al.*, 1989). At present, Cr and Pt layers with a thickness of 1-2 nm can be produced by means of magnetron sputtering with almost no sub-structure observable at magnifications over 300000x both in TEM and SEM (Gross *et al.*, 1985, 1990; Hermann and Müller, 1991; Wergin *et al.*, 1993; Stokroos *et al.*, 1995, 1998). These latter authors claim that a 1-3 nm thin layer of Au/Pd, produced by magnetron sputtering devices, is without detectable sub-structure of the grains up till magnifications of 200000 times. Wepf *et al.* (1991) used a combination of Pt/Ir/C in transmission and scanning transmission electron microscopy (TEM/STEM) and SEM investigations on freeze-dried macromolecules and claim that the structure of the coating does not change after the sample is exposed to air, in contrast to coatings of Ta/W and Pt/C. For *non-coating* fixed samples there is no need for an external metal coating.

Cryofixation

Preservation with cryoprotectant infiltration.

Besides high pressure freezing, where the initiation of small crystal nuclei is retarded, the initiation of ice crystals can be disturbed by infiltration of a cryoprotectant, such as glycerine, sucrose, dimethylsulfoxide (DMSO), polyethylene glycol (PEG), polyvinyl pyrrolidone (PVP), dextrans, hydroxy-ethyl starch, acetone, *t*-butanol, etc. Particularly PEG and PVP are polymeric agents of the so-called non-penetrating type and mainly envelope the tissue rather than penetrate the structure; their effect is not fully understood. These high molecular weight compounds can very well bind water, reducing the amount of free water. The prevention of freezing outside the cell possibly delays the freezing inside the cell (Echlin and Burgers, 1977). There is, however, an important condition with the selection of cryoprotectant. When an FE-SEM is used, the cryoprotectant should not evaporate in the high vacuum of the microscope and so not pollute the sample or the environment of the specimen stage. When the cryoprotectant is removed before investigation in the FE-SEM pollution is largely avoided. If the cryoprotectant molecules are too large, impregnation is hampered and there is no protection against ice crystal damage (Zhang and Rawson, 1996). Moreover the osmotic value of the cryoprotectant should be approximately the same of that of the tissue, otherwise damage to tissues and cells occurs.

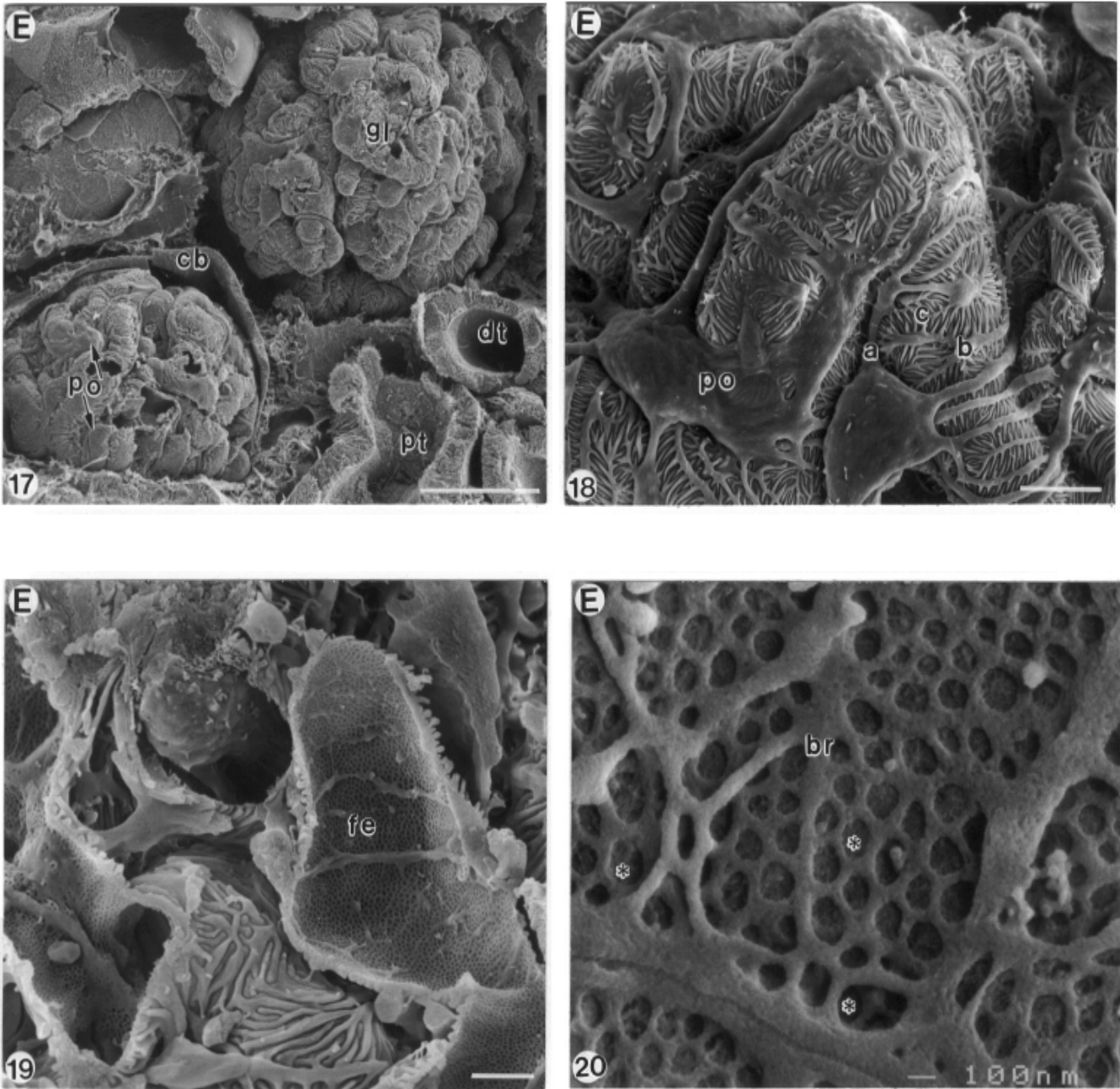
A disadvantage of using a cryoprotectant is the fact that all open spaces are filled with it, and depending on their size the presence of its particles can disturb the view onto the structure. Another disadvantage is the dif-

ficulty to sublime the ice in between the various sub-structures such as microvilli. Sucrose treated samples show a good example of this effect, because no sublimation of ice on the sample surface is possible. Thus a slightly more flat and dull image results. Moreover, smearing out of the cryoprotectant can occur, which makes it more difficult to observe image details at the surface of the specimen. According to Dubochet *et al.* (1987), the natural cryoprotectants present can defend the structures against ice-crystal damage for a distance of only 10 mm from the cooling face, while with incubation of cryoprotectants the structure should be free of crystalline ice over a distance of approximately 30-40 mm.

A 25-30 % aqueous glycerol solution depresses both the equilibrium freezing temperature and the ice nucleation, giving a good protection against ice crystal formation and growth. Fractures through glycerol infiltrated frozen tissue at variance with those non-protected tissues often run along the plane of membranes exposing the cytoplasmic organelles.

Freeze drying of biological tissue is a good alternative to critical point drying. Because freezing from water is difficult for obvious reasons, *t*-butanol is used as freezing medium. FD samples were always GA/TAO or GA/OTOTO fixed prior to freezing from *t*-butanol. In our cryo-FE-SEM experiments we have used *t*-butanol in various concentrations as a cryoprotectant in combination with standard GA fixation only. The tissue was not postfixed, but after pre-fixation infiltrated with *t*-butanol and fast frozen. Of course this is different from the mild GA fixation employed with and without glycerol as cryoprotectant. It is a compromise between cryopreparation and FD. After freezing the *t*-butanol was allowed to sublime while still frozen, whereafter the frozen sample was fractured, coated and investigated in the frozen state. Whether the *t*-butanol as a higher alcohol attacks (has a slightly dissolving effect on) the surface of the sample after prolonged contact during infiltration is not clear. Samples appear smoother than the chemical (non-coating) fixed ones after dehydration/drying. We were surprised by the similarity between the cryo- and *non-coating* images with respect to their fracturing behavior.

Preservation with a preliminary very mild pre-fixation. Another way to reduce the effects of ice-crystal damage is a very light *pre-fixation with GA*, carried out as perfusion fixation in animal experiments or as immersion fixation of human material. In this case the mild fixation serves mainly to give some rigidity to the tissue in order to get vibratome of approximately 100 mm thickness. A similar short fixation is carried out in immuno-electron microscopy to preserve at least some



Figures 17-20. Type E: Tissue frozen with 30-100% *t*-butanol cryoprotectant infiltration after standard 2% GA pre-fixation, *t*-butanol removed by sublimation, prior to SEM observation. **Figure 17.** Kidney tissue with two glomeruli (gl), showing the capsule of Bowman (cb), the podocytes (po), distal (dt) and proximal (pt) tubulus cells; bar = 21 mm = 10 μ m. **Figure 18.** Detail of podocyte body (po) with primary (a), secondary (b) and tertiary (c) extensions; bar = 14 mm = 2 μ m. **Figure 19.** Overview of fenestrated capillary endothelium (fe); bar = 11 mm = 5 μ m. **Figure 20.** Detail of fenestrated endothelium with thickened branches (br), note substructure (*) inside the fenestrae; the image appearance is comparable with TAO non coating results, bar = 5 mm = 100 nm.

of the structure. A mild fixation can be carried out in combination with the infiltration of a so-called penetrating protectant, such as glycerol, dimethyl sulfoxide, methanol, ethanol, ethylene-glycol, acetone or *t*-butanol. The mild fixation takes care of the permeabilization of the structure for the infiltration of the cryoprotectant. Tissues are then treated according the “grid-method“ described above.

The “grid-method“ allows (light-microscopic) sections to be handled and frozen, so ice-crystal damage is minimized at least in the area which was close to the cold face of the mirror. Sublimation of the ice at the surface of the fracture is carried out at -100 to -110°C, because at lower temperatures (< -120°C) the sublimation process is slowed-down too much to be practical; sublimation at higher temperatures (>-90°C) can cause ice-crystallization again. The sublimation time is important in that, long sublimation times can dry the sample surface, damaging the structure. The sublimation time and temperature should be chosen in such a way that sufficient relief is observable to distinguish the various cell organelles, e.g., membranes. When the etching or sublimation time is too short the structures are too much embedded in ice, so differentiation between cell organelles becomes difficult. We used an average sublimation time of 60-90 seconds at -110°C.

Comparison of images

In general the cryo-FE-SEM image, obtained after a preliminary glutaraldehyde fixation (in combination with a cryoprotectant treatment), and the TEM image, obtained after standard fixation, showed the most resemblance. In the cytoplasm, cell organelles such as mitochondria, vesicles, cell nuclei and endoplasmic reticulum were well observable in cryo-FE-SEM images and TEM ultra-thin sections after chemical fixation; this also holds for cell borders. In the cryo-FE-SEM image, they can be observed because of the open spaces which exist when the ice sublimates; in TEM images they can be seen as space filled up with embedding medium. In the cryo-FE-SEM image, slightly more relief can be observed, in contrast to the TEM image which is completely flat.

The *non-coating* treated and afterwards critical-point dried tissue in the FE-SEM of course has a much more three-dimensional appearance. But the chemically fixed, dehydrated and finally critical-point dried sample, gave a slightly rougher fracture face. The cryo image seems more “crisp“ compared to both the non-coating FE-SEM and standard TEM images. Possibly the formation of osmium complexes, caused some thickening of those structures. In more complex structures such as a glomerulus this is different. Both the FE-SEM images obtained after cryo fixation and non coating treat-

Figures 21-26. Type F. Tissue fixed by means of the standard GA-Tannic acid-Arginine-OsO₄ non coating procedure, dehydration and CPD. Compared to the cryo-images of Figures 1-16, taken at 5-10 kV, all images of Figures 21-26 have been investigated at 2 kV. **Figure 21.** Part of glomerulus with podocyte body (po) and capsule of Bowman (cb); compare with Figure 17; bar = 14 mm = 10 μm. **Figure 22.** Highly branched network of podocyte body with primary (a), secondary (b) and tertiary (c) extensions; bar = 10 mm = 10 μm. **Figure 23.** Detail of fenestrated capillary endothelium with thickened branches, note the difference with Figure 20; bar = 25 mm = 1 μm. **Figure 24.** Distal (dt) and proximal (pt) tubular cell, the last one with microvilli (mi), note globular particles inside lumen of proximal cell; bar = 18 mm = 10 μm. **Figure 25.** Other view on proximal tubular cell, with microvilli (mi) and plasma membrane infolding (if); bar = 18 mm = 2 μm. **Figure 26.** Detail of epithelial wall of a distal tubular cell covered with microvilli (mi); bar = 33 mm = 10 μm.

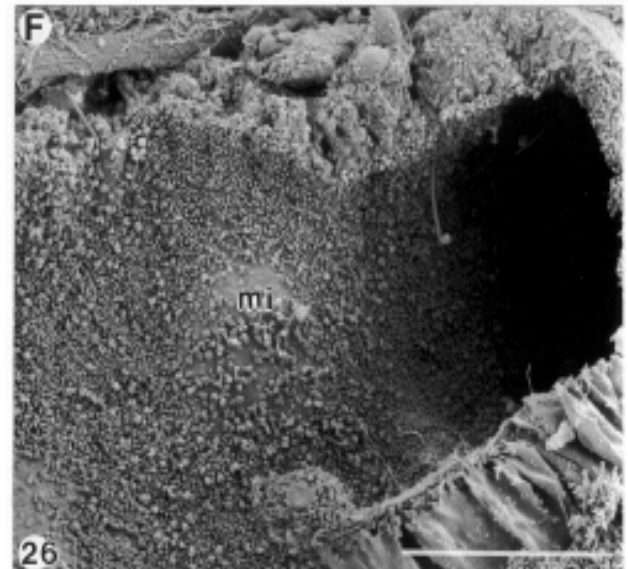
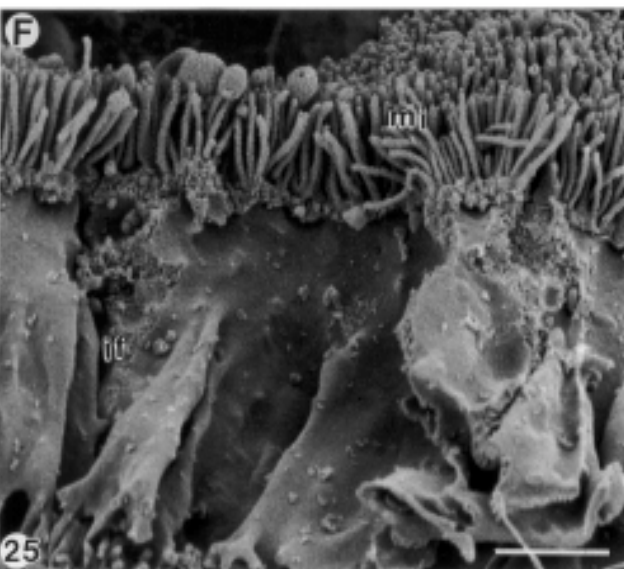
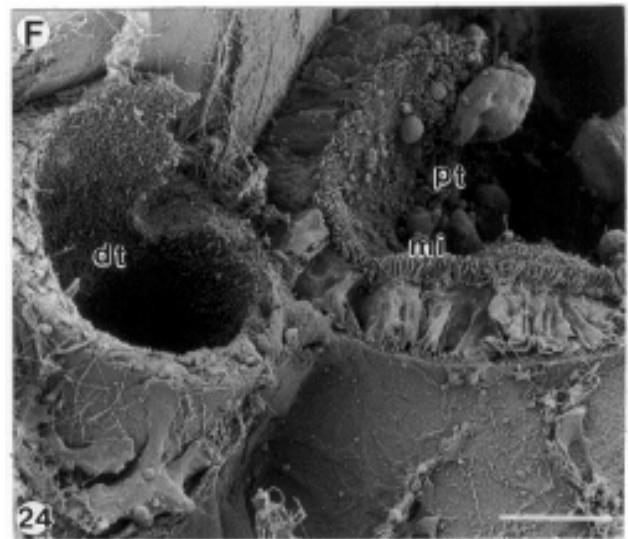
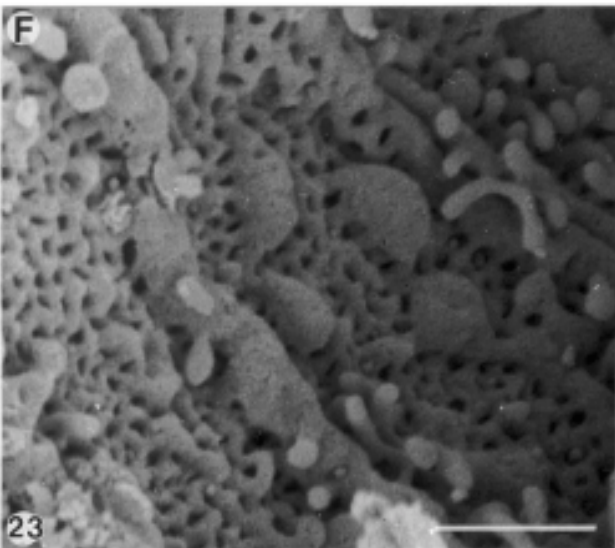
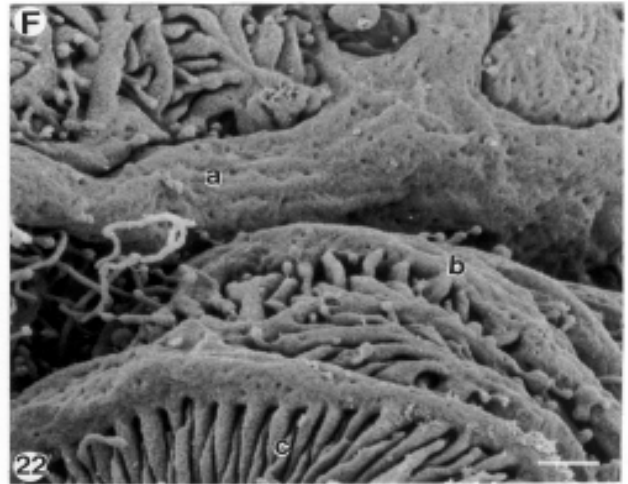
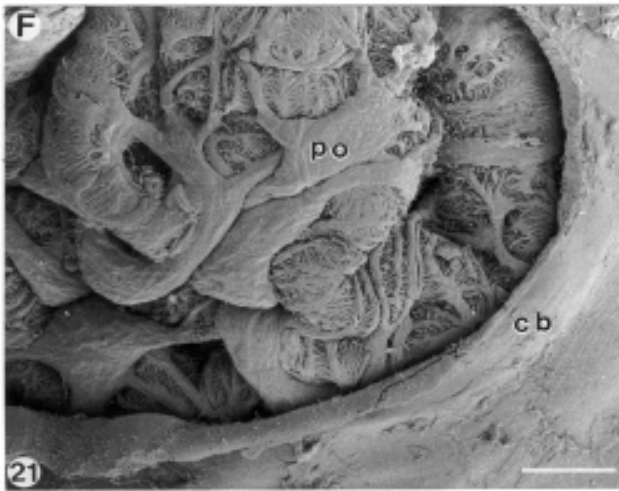
ment respectively are superior in quality to the FE-SEM images obtained after standard GA/OsO₄ fixation. Part of the fenestrated endothelium in relation to the basal membrane and the fractured podocytes can be observed in the cryo-FE-SEM image and facilitates interpretation of the image. The same fenestrated endothelium is also visible in three dimensions in the non-coating fixed sample. Similar to the observation made in the non-coating images of the proximal tubulus, a thickening of those structures occurs as a result of the bound osmium.

Conclusions

1. Cryo-FE-SEM of tissue is a powerful tool for morphological investigations; it is a fast and reliable method where ice-crystal damage can be minimized. Images sometimes are difficult to interpret due to the variance of fracture faces occurring at different cryoprotectant treatments. Removal of the cryoprotectant prior to SEM observation is recommended. High accelerating voltages are not used in cryo-SEM because the secondary emission coefficient of ice at 5-10 kV is not significantly lower than that at 10-25 kV. Moreover, the quality of poorly prepared specimens is lowered even more by the high vacuum (< 10⁻⁹ Torr) of the microscope. Cryo-FE-SEM images show rather good resemblance with TEM images of tissue sections and freeze fracture replicas in showing the cytoplasmic contents, but of course they have a three-dimensional appearance.

2. Non-coating FE-SEM of tissue is a powerful tool for morphological investigations; it is a very reliable method, minimizing artefacts due to extraction of tissue components and severe volume changes. Detailed sam-

Cryopreparation for FESEM



ple surface information can be obtained when the specimen is observed at low accelerating voltages. Non-coating and cryo-FE-SEM images are sometimes similar and sometimes complementary in information; both methods should be employed in combination.

3. Cryo specimens prepared without cryoprotectant, show too much freezing damage; *t*-butanol is a good alternative for glycerol and can keep down freezing damage to an acceptable level. Recent experiments in our laboratory have, however, shown that treatment with methanol as a cryoprotectant (20-30%) is an even better alternative, because removal by sublimation is easier, while methanol acts as a simple fixative as well. A mild GA-pre-fixation prior to freezing facilitates the production of thin vibratome sections suitable for cryo-experiments and reduces freezing damage as well.

4. There is no clear answer to the question which method (cryo-FE-SEM, *non-coating* FE-SEM or TEM) is the most appropriate one for tissue investigation, because they often give complementary results or information. The method to prevail is slightly dependent on the type of tissue to be investigated. It can be recommended most of the time to use both cryo- and *non-coating* preparation methods to obtain three-dimensional and cytoplasmic information from the same specimen. Cryo-FE-SEM information is almost similar to TEM information of tissue ultra-thin sections and much easier to obtain. If one allows a light prefixation of human tissue immediately after excision, cryo-FE-SEM can be employed for surgical samples for diagnostic purposes.

References

- Adrian M, Dubochet J, Lepault J, McDowell A (1984) Cryo-electron microscopy of viruses. *Nature (London)* **308**: 32-36.
- Allenspach A (1993) Ultrastructure of early chick embryo tissue after high pressure freezing and freeze substitution. *Microsc Res Techn* **24**: 369-384.
- Ansell P, Capers M (1989) A review of field emission electron microscopy. *Eur Microsc Analysis* **33**: 26-28.
- Apkarian RP (1994) Analyses of high quality monatomic chromium films used in biological high resolution scanning electron microscopy. *Scanning Microsc* **8**: 289-301.
- Boyde A, Maconnachie E (1979) Volume changes during preparation of mouse embryonic tissue for scanning electron microscopy. *Scanning* **2**: 149-163.
- Carr KE, Hayes TL, McKoon M, Sprague M, Bastacky SJ (1983) Low temperature scanning electron microscope studies of mouse small intestine. *J Microsc* **132**: 209-217.
- Chaplin AJ (1985) Tannic acid in histology, a historical perspective. *Stain Techn* **60**: 219-231.
- Dubochet J, Adrian, Chang J-J, Lepault J, McDowell AW (1987) Cryo-electron microscopy of vitrified specimens. In: *Cryo-Techniques in Biological Electron Microscopy*. Steinbrecht RA, Zierold K (eds). Springer Verlag, Berlin, pp 114-131.
- Dubochet J, Richter K, Roy H-V, McDowell A (1991) Freezing: Facts and hypothesis. *Scanning Microsc Suppl* **5**: 11-16.
- Dunnebie EA, Segenhout JM, Kalicharan D, Jongebloed WL, Wit HP, Albers FWJ (1995) Low voltage field emission microscopy of non coated guinea pig hair cell stereocilia. *Hear Res* **90**: 139-148.
- Echlin P, Burgess A (1977) Cryofracturing and low temperature scanning electron microscopy of plant material. *Scanning Electron Microsc* 1977: 491-500.
- Echlin P (1978) Low temperature scanning electron microscopy: a review. *J Microsc* **112**: 47-61.
- Echlin P (1992) *Low Temperature Microscopy and Analysis*. Plenum Press, New York.
- Edelmann L (1994) Low temperature embedding of chemically unfixed biological material after cryosorption freeze-drying. *Scanning Microsc* **8**: 551-552.
- Finch GL, Bastacky SJ, Hayes TL, Fisher GL (1987) Low temperature scanning electron microscopy of particle-exposed mouse lung. *J Microsc* **147**: 193-203.
- Frederik PM, Stuart PH, Boman PHH, Busing WM (1989) Phospholipid: Nature's own slide and coverslip for cryo-electron microscopy. *J Microsc* **153**: 81-92.
- Gilkey JC, Staehelin LA (1986) Advances in ultra-rapid freezing for the preservation of cellular ultra-structures. *J Electron Microsc Techn* **3**: 177-210.
- Gross H, Müller T, Wildhaber I, Winkler H (1985) High resolution metal replication quantified by image processing of periodic test specimens. *Ultramicroscopy* **16**: 287-304.
- Gross H, Krusche K, Tittman P (1990) Recent progress in high resolution shadowing for biological transmission electron microscopy. *Proc XIIth Int Congr Electron Microsc*, vol 1. Peachey LD, Williams DB (eds). San Francisco Press, San Francisco. pp. 510-511.
- Guggenheim R, Duggelin M, Mathys D, Grabski C (1991) Low-temperature SEM for detection of fungicide activity. *J Microsc* **161**: 337-342.
- Hermann R, Müller M (1991) High resolution biological scanning electron microscopy: a comparative study of low temperature metal coating techniques. *J Electr Microsc Techn* **18**: 440-449.
- Hermann R, Müller M (1993) Progress in scanning electron microscopy of frozen-hydrated biological samples. *Scanning Microsc* **7**: 343-350.

- Hohenberg H, Mannweiler K, Müller M (1994). High pressure freezing of cell suspensions in cellulose capillary tubes. *J Microsc* **175**: 34-43.
- Humbel B, Müller M (1986) Freeze substitution and low temperature embedding. In: *The Science of Biological Specimen Preparation*. Müller M, Becker RP, Boyde A, Wolosewick JJ (eds). Scanning Electron Microscopy Inc, AMF O'Hare (Chicago, IL). pp. 175-183.
- Humphreys SH (1989) Freeze-fracture of manufactured foods. *J Electron Microsc Techn* **13**: 300-308.
- Inoué T (1985) High resolution scanning electron microscopic cytology. Specimen preparation and intracellular structures observed by scanning electron microscopy. In: *The Science of Biological Specimen Preparation*. Müller M, Becker RP, Boyde A, Wolosewick JJ (eds). Scanning Electron Microscopy Inc, Chicago, pp. 245-256.
- Inoué T, Koike H (1986) A new cryo-scanning electron microscopy for observing intracellular structures of non-fixed biological tissues. *Proc XIth Int Congress Electron Microsc*. Imura T, Maruse S, Susuki T (eds). *Jpn Soc Electron Microsc*, Tokyo. pp. 2227-2228.
- Jongebloed WL, Kalicharan D (1992) The use of OTOTO, GOTO and GOTU non coating techniques on kidney, liver and lung tissue of the rat examined by TEM. *Beitr Elektronenmikroskop Direktabb Oberfl* (Ehrenwerth U, ed). Verlag RA Remy, Münster. **25**: 351-358.
- Jongebloed WL, Kalicharan D, Los LI, Worst JGF (1992a) Study of the substructure of the Morgagnian and Brunescens cataract with TAO non coating technique. *Doc Ophthalmol* **82**: 154-168.
- Jongebloed WL, Kalicharan D, Vissink A, Konings ATW (1992b) Application of the OTOTO non-coating technique; a comparison of LM, TEM, and SEM. *Microscopy and Analysis* **28**: 31-33.
- Jongebloed WL, Kalicharan D, Worst JGF (1993a) The microscope in ophthalmological research. *Microscopy and Analysis* **25**: 5-7.
- Jongebloed WL, Kalicharan D, Los LI, Worst JGF (1993b) The Morgagnian and Brunescens cataract morphology studied with SEM and TEM. *Eur J Morphol* **31**: 97-102.
- Jongebloed WL, Kalicharan D (1994) Tannic acid/arginine/osmium tetroxide fixation of rat tissue by the microwave procedure. *Beitr Elektronenmikroskop Direktabb Oberfl*. Ehrenwerth U (ed). Verlag RA Remy, Münster, **27**: 243-252.
- Jongebloed WL, Kalicharan D, Worst JGF (1994) High resolution FEG-SEM images of biological tissue. *Proc 13th Int Conf Electron Microsc* (Paris). Jouffrey B, Colliex C, Hernandez-Verdun D, Schrevel J, Thomas D (eds). *Led Éditions de Physique*, Paris. Vol. 3a, pp. 777-778.
- Jongebloed WL, Kalicharan D (1996) Low voltage visualization of glycocalyx (-like) structures at various biological tissues. *Beitr Elektronenmikroskop Direktabb Oberfl*. Ehrenwerth U (ed). Chr. Ehrenwerth, Münster. **29**: 201-212.
- Jongebloed WL, Dunnebier EA, Kalicharan D, Albers FWJ (1996) Demonstration of the fine structure of stereocilia in the organ of Corti of the guinea pig by field emission scanning electron microscopy. *Scanning Microsc* **10**: 147-164.
- Kalab M (1993) Practical aspects of electron microscopy in dairy research. *Food Structure* **12**: 95-114.
- Kalicharan D, Jongebloed WL, Los LI, Worst JGF (1992) Application of tannic acid non-coating technique in eye research: lens capsule and cataractous lens fibres. *Beitr Elektronenmikroskop Direktabb Oberfl*. Ehrenwerth U (ed). RA Remy Verlag, Münster, **25**: 201-205.
- Kok LP, Boon ME (1992) *Microwave Cookbook for Microscopists*. Coulomb Press, Leiden.
- Login GR, Dvorak AM (1994a) *The Microwave Toolbook, a Practical Guide for Microscopists*. Beth Israel Hospital, Boston MA.
- Login GR, Dvorak AM (1994b). New methods of microwave fixation for microscopy. A review of research and clinical applications 1970-1992. In: *Progress Histochem Cytochem* 27/4. Graumann W, Lojda Z, Pearse AGE, Schieber TH (eds). Gustav Fischer Verlag New York.
- Los LI, Kalicharan D, Jongebloed WL, Van Rij G, Worst JGF (1992) Evaluation of various post-fixation agents on the sheep vitreous body; a SEM investigation of the fine structure. *Beitr Elektronenmikroskop Direktabb Oberfl*. Ehrenwerth U (ed). RA Remy Verlag, Münster, **25**: 359-364.
- Meissner DH, Schwartz (1990) Improved cryoprotection and freeze-substitution of embryonic quail retina: a TEM study on ultrastructural preservation. *J Electron Microsc Techn* **14**: 348-356.
- Menco BPhM (1986) A survey of ultra-rapid cryofixation methods with particular emphasis on applications to freeze-fracturing, freeze-etching, and freeze-substitution. *J Electron Microsc Techn* **4**: 177-240.
- Moor H (1987) Theory and practice of high pressure freezing. In: *Cryotechniques in Biological Electron Microscopy*. Steinbrecht RA, Zierold K (eds). Springer-Verlag, Berlin. pp 175-191.
- Müller MH, Meister N, Moor H (1980) Freezing in a propane jet and its application in freeze-fracturing. *Mikroskopie* **36**: 129-140.

- Murakami T (1974) A revised method for non-coated SEM specimens. *Arch Histol Jap* **36**: 189-193.
- Murphy JA (1978) Non-coating techniques to render biological specimens conductive. *Scanning Electron Microsc* 1978; III: 175-195.
- Plattner H, Bachman L (1982) Cryofixation: a tool in biological ultrastructure research. *Int Rev Cytol* **79**: 237-306.
- Reid N, Beesley J (1991) Sectioning and Cryo-sectioning for Electron Microscopy. *Practical Methods in Electron Microscopy*, vol. 13. Elsevier, Amsterdam.
- Robards AW, Sleytr UB (1985) Low Temperature Methods in Biological Electron Microscopy. *Practical Methods in Electron Microscopy*, vol. 10. Elsevier, Amsterdam.
- Robards AW, Abeyssekera RM (1992) Improved freeze preparation of biopolymer molecules for transmission electron microscopy. *Proc 10th Eur Congress Electron Microsc*. Megías-Megías L, Rodríguez-García MI, Ríos A, Arias JM (eds). Univ Granada Press. vol II, pp 77-78.
- Sargent JA (1986) Cryo-preservation for scanning electron microscopy avoids artifacts induced by conventional methods of specimen preparation. *Tissue & Cell* **18**: 305-311.
- Sargent JA (1988) Low temperature scanning electron microscopy: advantages and applications. *Scanning Microsc* **2**: 835-849.
- Sitte H, Edelmann L, Neumann K (1987) Cryofixation without pretreatment at ambient temperature. In: *Cryotechniques in Biological Electron Microscopy*. Steinbrecht RA, Zierold K (eds). Springer-Verlag, Berlin. pp. 87-113.
- Stokroos I, Kalicharan D, Jongebloed WL (1995) A comparative study of ultrathin coatings for high resolution FEG-SEM. *Beitr Elektronenmikr Direktabb Oberfl*. Ehrenwerth U (ed). Chr. Ehrenwerth, Münster. **28**: 165-172.
- Stokroos I, Kalicharan D, Van der Want JJJ, Jongebloed WL (1998) A comparative study of thin coatings of Au/Pd, Pt and Cr produced by magnetron sputtering for FE-SEM. *J Microsc* **189**: 79-89.
- Studer D, Michael M, Muller M (1989) High pressure freezing comes of age. *Scanning Microsc* **3**: 253-269.
- Talmon Y (1986) Imaging surfactant dispersions by electron microscopy of vitrified specimens. *Colloid Surf* **19**: 237-248.
- Van Aelst AC, Müller T, Dueggelin M, Guggenheim R (1989) Three-dimensional observation on freeze-fractured frozen hydrated *Papaver dubium* pollen with cryo-scanning electron microscopy. *Acta Bot Neerl* **38**: 25-30.
- Walther P, Hentschel, Herter P, Müller T, Zierold K (1990) Imaging of intramembranous particles in frozen hydrated cells (*Saccharomyces cerevisiae*) by high resolution cryo-SEM. *Scanning* **12**: 300-307.
- Wepf R, Amrein M, Burkli U, Gross H (1991) Platinum/iridium/carbon: a high resolution shadowing material for TEM, STM and SEM of biological macromolecular structures. *J Microsc* **163**: 51-64.
- Wergin WP, Erbe EF, Robins A (1993) Use of platinum shadowing and magnetron sputter coating in an Oxford Cryotransfer system to increase low temperature resolution of biological samples in a Hitachi field emission scanning electron microscope. *Proc 51st Ann Meeting Microsc Soc America [EMSA]*. Bailey GW, Rieder CL (eds). San Francisco Press, San Francisco. pp. 122-123.
- Willison JHM, Rowe AJ (1980) Replica, Shadowing and Freeze-Etching Techniques. *Practical Methods in Electron Microscopy*, Vol 8. North-Holland, Amsterdam.
- Zhang T, Rawson DM (1993) Cryopreservation of pre-hatched embryos of zebrafish (*Brachydanio-erio*). *Aquatic Living Resources* **6**: 145-153.
- Zhang T, Rawson DM (1996). Feasibility studies on vitrification of intact zebrafish (*Brachydanio-erio*) embryos. *Cryobiology* **33**: 1-13.

Discussion with Reviewers

G.M. Roomans: What is the function of NaNO₂ in the perfusion fluid?

Authors: NaNO₂ is added to the perfusion fluid as a vascular dilation agent, to avoid that blood vessels are distorted due to a temporary osmotic change. It is in particular known in neurobiological experiments with rather thin blood vessels.

G.M. Roomans: You included acrolein in the prefixative mixture, which is a nasty substance. What are the advantages of it and is it worth the risk ?

Authors: Acrolein in low concentrations (0.1-0.2%) enhances preservation by its faster penetration of the tissue compared to glutaraldehyde. Paraformaldehyde is a fast penetrating fixative as well, but does not give cross linking of the protein chains in three dimensions. In higher concentrations (> 0.5%) acrolein can cause adverse effects. We think acrolein is worth using, if necessary precautions for safety are taken.

R. Wróblewski: In total, seven methods of preparation are described. Only one of these is suited for X-ray microanalysis, but no method was mentioned as being the best choice.

Authors: In almost all cases osmium, a heavy element with many K, L and M lines interfering with especially lighter elements, was used in one way or another as a postfixative. This makes the use of these methods for X-ray microanalysis rather difficult. From our experiments we could state that [GA + TAO] or [GA + OTO(TO)] for FE-SEM use only is quite acceptable, but for TEM both methods are inferior. A prefixation with a mixture of GA, paraformaldehyde (PF), acrolein and picric acid is quite an improvement for both FE-SEM and TEM in combination with TAO or OTO(TO) respectively. This is particularly valid for combined research with FE-SEM and TEM. However, the best results for TEM are obtained, when postfixation is carried out with a mixture of OsO₄ and K₄Fe(CN)₆. On the other hand, this is not valid for all types of specimens, and one should compare the methods for the type of specimen/tissue under investigation to obtain an optimal result. It is therefore difficult to make statements about the value for each of the methods used.

A. Riva: The statement of the authors that tannic acid in combination with OsO₄ is not widely used, might not be valid for Japan where it is commonly employed.

Authors: We found that tannic acid is more effective after GA/PF prefixation only, than when OsO₄ is used prior to the introduction of tannic acid. However, tannic acid is used in methods called GOTO (glutaraldehyde, osmium tetroxide, tannic acid, osmium tetroxide) and GOTU (glutaraldehyde, osmium tetroxide, tannic acid, uranyl acetate) for SEM/TEM. The conductivity of samples prepared by the GOTO or GOTU methods, respectively, is inferior, so a conductive coating has to be applied.

A. Riva: Why are poorly prepared specimens more affected by high vacuum?

Authors: Poorly prepared specimens do not show the rigidity needed to withstand the forces exerted by drying and particularly in vacuum. There is a much greater chance that these specimens will collapse. Crosslinking of protein chains and stabilization of compounds make the sample stronger.

A. Riva: Why did the authors use lower voltages with *non-coated* samples than with the cryo-prepared samples?

Authors: At low voltage information about the surface of the sample is obtained. Low voltage is only possible when sufficient primary electrons can generate secondary electrons at beam incidence and sufficient back-scattered electron from the sample surface are available. The presence of osmium in the top layer of the sample, as a result of the non-coating method used, guarantees

that this is the case in FE-SEM. The secondary and backscatter coefficient of ice becomes considerably lower, when the accelerating voltage is lowered below 5 kV. There is an optimum at 5-10 kV, a much higher accelerating voltage is not useful either.

A. Riva: What is the rationale for using Au/Pd for coating?

Authors: When non-coating techniques are used, no external coating is required, except maybe for the GOTO and GOTU method as mentioned before. If a thin coating should be necessary, a 2-3 nm thin coating of Au/Pd is fine. Stokroos *et al.* (1998) have found that such an Au/Pd coating, prepared by most of the magnetron sputtering devices, has small enough grains so that no substructure is observed at least up to magnifications of 200000x in FE-SEM. Cr-coating has a still finer grain, so this can be used for ultra-high resolution work.